First-principles calculations of structural, electronic, and thermodynamic properties of Na_2BeH_4

C. H. Hu,[1,2] Y. M. Wang,[1,*] D. M. Chen,[2] D. S. Xu,[2] and K. Yang[2]
[1]*Shenyang National Laboratory for Materials Science, Institute of Metal Research, Chinese Academy of Sciences, 72 Wenhua Road, Shenyang 110016, People's Republic of China*
[2]*National Engineering Research Center, Institute of Metal Research, Chinese Academy of Sciences, 72 Wenhua Road, Shenyang 110016, People's Republic of China*
(Received 30 April 2007; revised manuscript received 10 August 2007; published 8 October 2007)

The plane-wave ultrasoft pseudopotential method based on the density-functional theory has been used to calculate the electronic structures of Na_2BeH_4. These calculations reveal that at ambient conditions, the crystal structure of α-Na_2BeH_4 at ground state is α-K_2ZnBr_4-type monoclinic (space group $P2_1/m$). With increasing pressure, the structural transition from α- to β-Na_2BeH_4 (α-Cs_2MgH_4 type, space group *Pnma*) occurs at 1.1 GPa accompanied with a volume reduction of 8.7%. The density of states and electron localization function analyses show that a stronger covalent-bonding interaction prevails in BeH_4 subunits and the crystals exhibit a nonmetallic feature. The relative thermal stability of α- to β-Na_2BeH_4 was further investigated by performing phonon calculations based on the density-functional perturbation theory. The calculated Helmholtz free energies and vibrational entropies show that α-Na_2BeH_4 is always kept more stable than β-Na_2BeH_4 with increasing temperature and is impossible to be transformed to the β phase.

DOI: 10.1103/PhysRevB.76.144104 PACS number(s): 31.15.Ew, 68.18.Jk

I. INTRODUCTION

Conventional hydrides, such as $LaNi_5$-H and $TiFe_{1.8}$-H, and Laves phase are inefficient to be applied as high-density solid-state reversible hydrogen storage materials due to their intrinsic limit of low gravimetric hydrogen density (GHD), although they exhibit good cycling performances under ambient conditions.[1] The complex hydrides composed of light non-transition-metal elements with high GHD are generally thought to be the most promising candidates. For example, the sodium alanate, $NaAlH_4$, and the magnesium alanate, $Mg(AlH_4)_2$, have 7.5 and 9.6 wt % theoretical hydrogen capacities, respectively. Accordingly, many attempts, such as transition-metal adding,[2] have been made to improve their poor hydrogenation kinetics. Recently, experimental and theoretical efforts[3–6] have been aimed toward this goal. However, the reversible release of only 3.0 wt % H below $T=373$ K for $NaAlH_4$ still cannot meet the FreedomCar standard of a gravimetric density of 5.0 wt% H.[7] Hence, it is in need of exploring other promising complex hydrides.

From the viewpoint of their high GHD, the complex alkyberyllium hydrides like Li_2BeH_4 (GHD: 15.0 wt %) and Na_2BeH_4 (GHD: 6.8 wt %) may be the possible candidates. Different from Li_2BeH_4, the crystal structure of which has been correctly indexed by Bulychev *et al.*,[8] the crystal structures of Na_2BeH_4 have not yet been characterized since their discovery a few decades ago,[9,10] and many experimental and theoretical questions about them remain. To our best knowledge, the valuable hint on Na_2BeH_4 can be found only in Ref. 11, in which the author assumed on the basis of crystal chemistry that one crystal structure would be an Al_2ZnO_4-type structure (orthorhombic, *Pnma*).

With technological progress in algorithms and computer hardwares, first-principles calculations based on the density-functional theory (DFT) with the use of the local density approximation (LDA) or generalized gradient approximation (GGA) can not only explain the already known properties of a given material but also resolve the ambiguities in experimental structural determination. This has made material design become realistic. Up to now, the theoretical prediction of crystal structures by using first-principles methods has been successfully applied to various materials such as C_3N_4,[12] $NaCdF_3$,[13] $Ca(AlH_4)_2$,[14] and Li_2NH.[15] Following in the footsteps of those works, we have performed the first-principles calculations of the pressure-induced structural transition and hydrogen adsorption and/or desorption properties of Li_2BeH_4.[16] After that, however, a question that arises is what are the properties of Na_2BeH_4 as one homologous hydride of Li_2BeH_4. To evaluate the structural transition of Na_2BeH_4, its crystal structure must be determined since it is still uncertain as mentioned above. In this light, its thermodynamic properties will be further discussed in the present work.

The paper is organized as follows: In Sec. II, we give the computational details. Then we present and discuss the calculated results in Sec. III. Finally, we draw our conclusions in Sec. IV.

II. COMPUTATIONAL DETAILS

All the total-energy calculations in this work were carried out using the plane-wave ultrasoft pseudopotential[17] (PW-USPP) method as implemented in the CASTEP code.[18] The PW91 form[19] of GGA and the CA-PZ form[20,21] of LDA were used to describe the exchange-correlation potential. The ionic positions, lattice parameters, and cell volumes were all relaxed within the algorithm[22] of Baranovskii, Efros, Gelmont, and Shklovskii (BEGS) by minimizing forces and stresses. To obtain the equilibrium geometries, the structural relaxations were performed without any constraint until the total energy was converged to 10^{-5} eV in the self-consistent loop and the force on each atom was smaller than 0.03 eV/Å. The convergence behavior (dependence of the total energy on the cutoff energy and the number of k points)

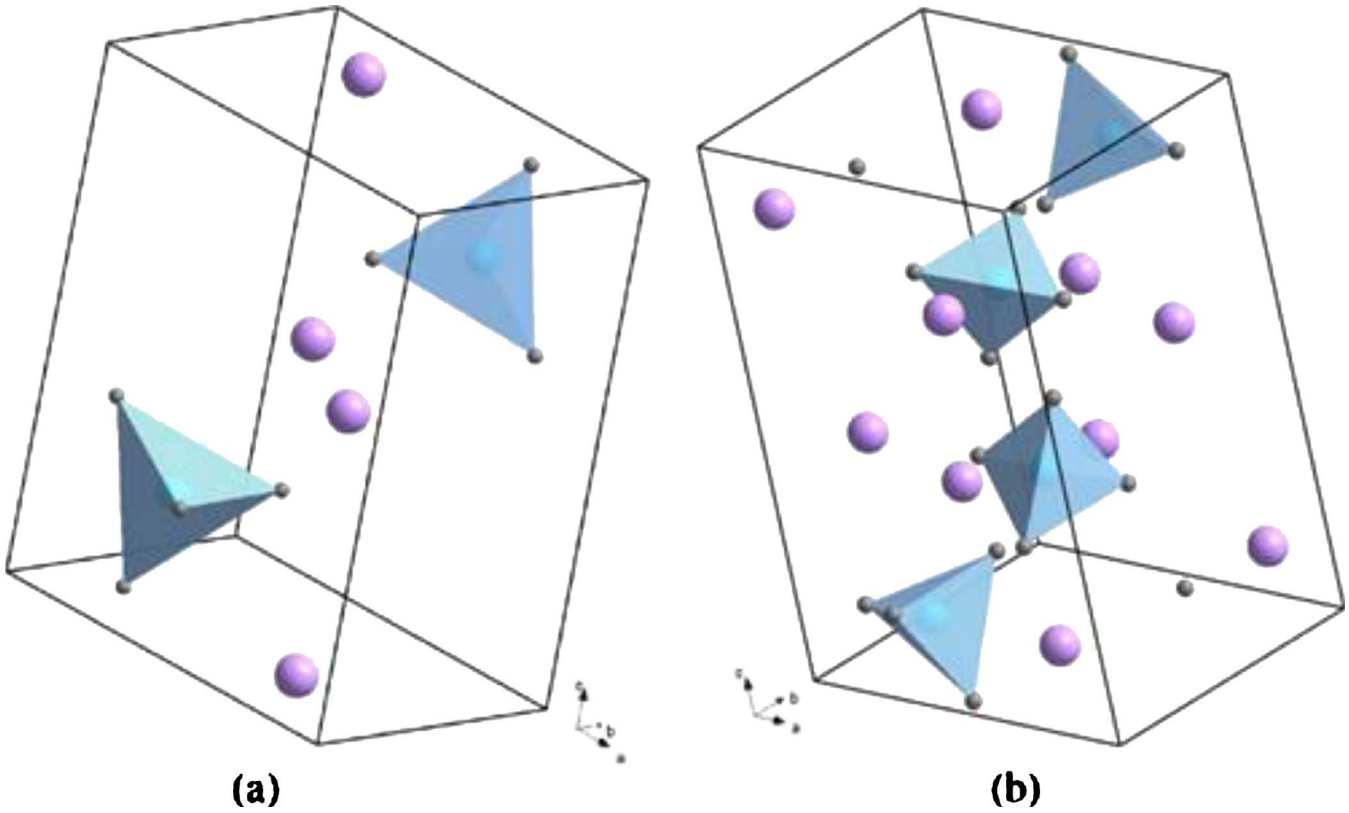

FIG. 1. (Color online) Crystal structure of (a) α-Na_2BeH_4 (α-K_2ZnBr_4, monoclinic-$P2_1/m$) and (b) β-Na_2BeH_4 (α-Cs_2MgH_4 type, orthorhombic-*Pnma*). The tetrahedra represent the BeH_4 subunits, in each of which the Be atom locates in the center and the four H atoms at its vertices.

was carefully examined for all the proposed crystal structures of Na_2BeH_4. Finally, the cutoff energy was chosen to be 380 eV and the k-point spacing smaller than 0.04 $Å^{-1}$ to guarantee that all the computational results either on the cutoff energy or on the number of k points converged to be on the order of meV. On the basis of these results, for the Na_2BeH_4 with closely related atomic arrangements and tiny total-energy differences, the relative thermal stabilities and vibrational and thermodynamic properties were discussed by performing phonon calculations based on the density-functional perturbation theory[23] (DFPT) using the PWSCF code.[24]

III. RESULTS AND DISCUSSION

In order to predict precisely its ground-state crystal structure, we performed the total-energy calculations for 11 trial structures with closely related atomic arrangements. They are, namely, α-Li_2BeH_4 (monoclinic, $P2_1/c$),[8] α-Cs_2MgH_4 (orthorhombic, *Pnma*),[25] β-Cs_2MgH_4 (tetragonal, $I4/mmm$),[26] Li_2BeF_4 (trigonal, R-3),[27] α-Na_2SO_4 (trigonal, P-$3m1$),[28] β-Na_2SO_4 (orthorhombic, *Fddd*),[29] K_2WO_4 (monoclinic, $C2/m$),[30] Ag_2WO_4 (orthorhombic, *Pnn*2),[31] Al_2MgO_4 (cubic, Fd-$3m$),[32] α-K_2ZnBr_4 (monoclinic, $P2_1/m$),[33] and β-K_2ZnBr_4 (monoclinic, $P2_1$),[33] respectively. As displayed in Fig. 1, except for the β-Cs_2MgH_4-type structure, BeH_4 forms an almost regular tetrahedral subunit with a Be atom at its center and four H atoms at its vertices, and Li atoms locate in interstices of the structure composed of those BeH_4 subunits.

All these hypothetical structures were optimized at ambient pressures, and the optimized volumes (V_0) and the total-energy differences (ΔE_0) per formula unit (f.u.) between them and the ground-state total energy of α-K_2ZnBr_4 as a reference were summarized in Table I. In this work, the total-energy calculations based on LDA and GGA were carried out respectively to evaluate the predicted reliability by these two approximations. As listed in Table I, no matter what is based on LDA or GGA calculations, the α-K_2ZnBr_4-type structure [hereafter, α-Na_2BeH_4; see Fig. 1(a)] is on the lowest energy, indicating that it is energetically the most favored structure at ground state. For GGA calculations, the same conclusion can be drawn that the total energies of α-Na_2BeH_4 are about 14.7 and 56.8 meV/f.u. lower than those of the second and third stable phases, α-Cs_2MgH_4-type and α-Li_2BeH_4-type structures. Such low total-energy differences foreshow that the phase transition among these three phases would occur once external thermodynamic conditions like pressure and temperature are changed. These results motivate us to investigate the stability of these possible Na_2BeH_4 structures at different pressures or temperatures. However, in subsequent calculations, only GGA was adopted since the ground-state total-energy differences obtained using LDA and GGA had a similar variational tendency, but GGA gives excellent atomic ground-state energies and significantly improves bond

TABLE I. Calculated volume V_0 (Å^3/f.u.) and the ground-state total-energy difference ΔE_0 (meV/f.u.) at ambient pressures using LDA and GGA.

	LDA		GGA	
Hypothetical modeling	V_0 (Å^3/f.u.)	ΔE_0^{LDA} (meV/f.u.)	V_0 (Å^3/f.u.)	ΔE_0^{GGA} (meV/f.u.)
α-K_2ZnBr_4	77.453	0	86.647	0
α-Li_2BeH_4	79.718	98.6	86.836	56.8
α-Cs_2MgH_4	69.649	70.9	74.254	14.7
β-Cs_2MgH_4	62.884	641.6	64.178	1025.3
α-Na_2SO_4	75.263	223.9	79.391	241.5
β-Na_2SO_4	74.902	125.5	80.223	158.8
Li_2BeF_4	85.659	320.1	98.814	349.7
Ag_2WO_4	78.652	290.4	85.563	320.8
Al_2MgO_4	70.325	874.5	74.664	1142.9
K_2WO_4	72.332	128.3	76.633	190.1

lengths of small molecules as demonstrated in previous papers, which may be appropriate for the calculations of Na_2BeH_4 containing a small subunit BeH_4. As listed in Table I, the total energies of β-Cs_2MgH_4-type, Li_2BeF_4-type, Ag_2WO_4-type, and Al_2MgO_4-type structures are quite higher than that of α-Na_2BeH_4, and their ΔE_0's reach 1025.3, 349.7, 320.8, and 1142.9 meV/f.u., respectively, indicating that these structures are much less stable and, thus, not considered in our following analyses. In addition, the total energy of β-K_2ZnBr_4-type structure is very close to that of α-Na_2BeH_4 and its final space group is $P2_1/m$ after performing the optimized calculation on its degraded structure with P_1 symmetry. Hence, it could also be excluded in our further discussion.

Due to the limit of computational cost, we do not perform a further verification of the full-potential linearized augmented plane waves (FLAPW) and the all-electron projector augmented waves (PAW) approaches. In fact, the extensive comparisons among the PW-USPP, FLAPW, and PAW approaches have been established for a variety of small molecules and bulk crystals. These comparisons indicated that, in most cases, these three approaches give virtually identical results.[34,35] The differences between the PW-USPP and the PAW or FLAPW approaches appear only in those materials such as some ferro- and antiferromagnetic systems and early $3d$ transition metals, in which the linearization of the valence-core exchange interaction is not negligible.[34–36] Our present system, however, is composed of only s,p-bonded main-group elements; it is expected that the reliable results could be obtained by PW-USPP. In addition, in our calculations, the contribution from the van der Waals (vdW) force is also negligible. The vdW force belongs to weak intermolecular bonds; it plays an important role only in those nonchemically weak bonded systems or molecules such as H_2, N_2, H_2O, and HCl.[37] Actually, previous theoretical calculations,[38] together with our calculations on Li_2BeH_4 (Ref. 16) and $Mg(AlH_4)_2$, have proven that the stronger covalent bondings between Al-H in AlH_4 subunits and between Be-H in BeH_4 subunits are mainly responsible for the relative stability of these complex hydrides.

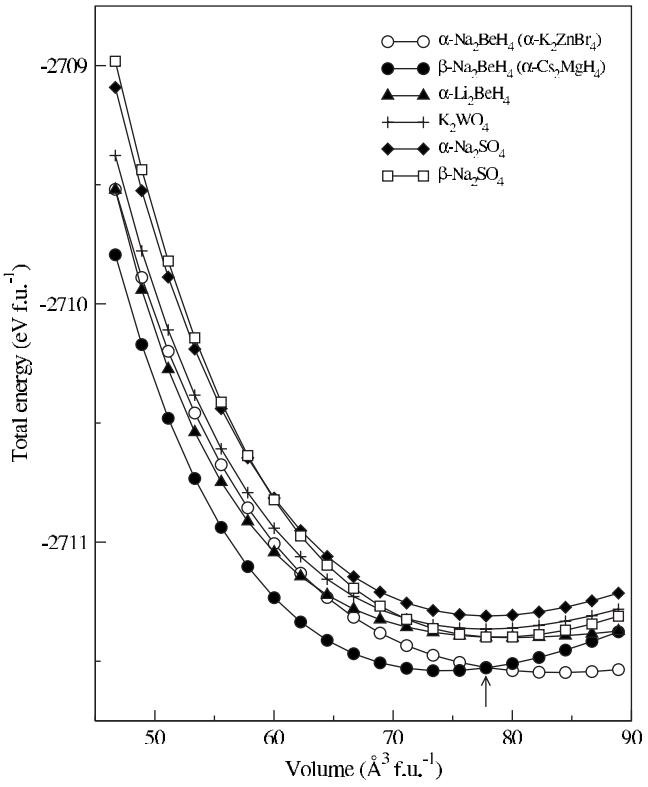

FIG. 2. Total energy (in eV/f.u.) versus the atomic volume (in Å^3/f.u.) for α-Na_2BeH_4 and the proposed structures. The $\alpha \rightarrow \beta$ structural transition point is marked with an arrow.

To theoretically determine at which volumes the crystal transitions occur for α-Na_2BeH_4 and the additional five proposed structures with the lower ΔE_0, we fitted their total-energy curves as a function of volume (E-V curves) using the Birch-Murnaghan equation of state[39] (BM-EOS) as plotted in Fig. 2. Then their behaviors are discussed. Figure 2 shows that when the volume is compressed to 78.4 Å^3/f.u., the E-V curve for α-Na_2BeH_4 intersects that of α-Cs_2MgH_4-type structure [hereafter, β-Na_2BeH_4; see Fig. 1(b)], indicating that a structural transition from α to β phase ($\alpha \rightarrow \beta$) would be undergone at this volume. Further compressing the volume, however, no other intersection point is found. This means that only one phase transition occurs at the pressure corresponding to this volume. The calculated equilibrium lattice parameters, internal atomic positions, bulk moduli (B_0), and corresponding pressure derivatives (B_0') for α- and β-Na_2BeH_4 were all compiled in Table II. We can find from the calculated B_0 that Na_2BeH_4 is an easily compressible material similar to Li_2BeH_4 (Ref. 16) and $Mg(AlH_4)_2$.[40]

Generally, comparing the Gibbs free energies (G) of different phases can help us get more accurate information on the structural transition point. However, our calculations were performed at temperature T=0 K; $G=E+PV-TS$ is just equal to the enthalpy $H=E+PV$. In this paper, the calculated enthalpy difference (H_β-H_α) versus pressure (P) relation, together with the volume-pressure (V-P) curve, was obtained by using the BM-EOS and presented in Fig. 3. The H_β-H_α

TABLE II. Optimized structural parameters: lattice constants (in Å), internal atomic positions (in fractional coordinates), bulk moduli B_0 (in GPa), and pressure derivatives B_0' for α-Na_2BeH_4 (α-K_2ZnBr_4 type) and β-Na_2BeH_4 (α-Cs_2MgH_4 type).

Structure	Lattice constant	Internal atomic position	B_0	B_0'
α-Na_2BeH_4	a=5.094	Na1: 0.7341, 0.2500, 0.5247	14.0	4.65
($P2_1/m$)	b=5.002	Na2: 0.7311, 0.2500, 0.0249		
	c=6.872	Be: 0.2777, 0.2500, 0.2219		
	β=98.4633	H1: 0.0628, 0.2500, 0.3368		
		H2: 0.4451, 0.4779, 0.2654		
		H3: 0.8138, 0.7500, 0.9853		
β-Na_2BeH_4	a=6.628	Na1: 0.1518, 0.2500, 0.4191	25.1	4.32
($Pnma$)	b=5.061	Na2: 0.4976, 0.2500, 0.6807		
	c=8.854	Be: 0.2290, 0.2500, 0.0833		
		H1: 0.3039, 0.0185, 0.1564		
		H2: 0.1963, 0.0034, 0.6564		
		H3: 0.6963, 0.5185, 0.8437		

becomes negative in this figure once the external pressure is beyond 1.1 GPa, from which the transition pressure (P_T) from α to β phase is established. From the P-V relation between α- and β-Na_2BeH_4 shown in the same figure, we can find that the volume is contracted to about 8.7% at the structural transition point, which is comparable to the results on Li_2BeH_4 (Ref. 16) and $Mg(AlH_4)_2$.[40] Such large volume shrinkages accompanied with the pressure-induced structural transition have been observed in high-pressure x-ray powder diffraction studies.[41,42]

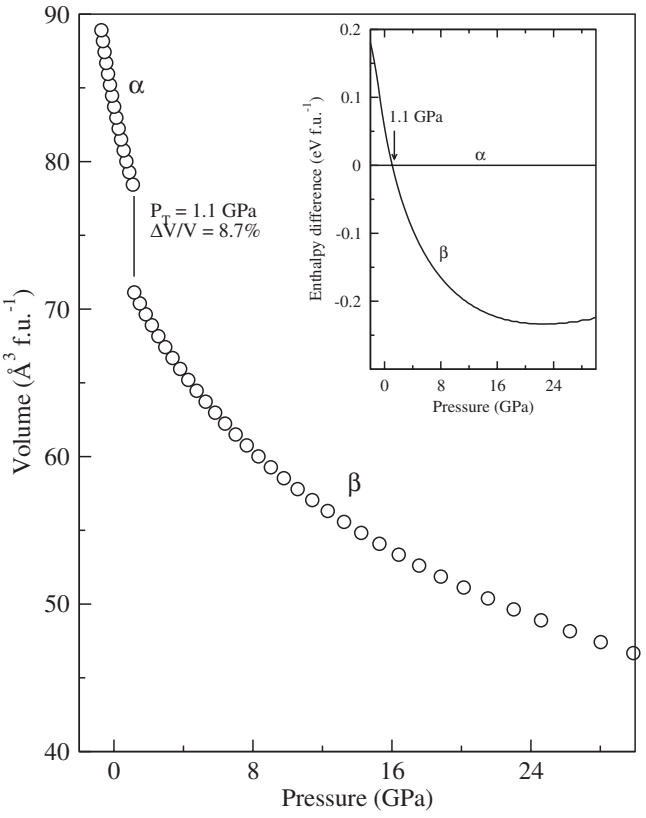

FIG. 3. Calculated pressure dependence on volume for α- and β-Na_2BeH_4. The enthalpy difference between α- and β-Na_2BeH_4 is shown in the inset.

The calculated DOS for α-Na_2BeH_4 at equilibrium was presented in Fig. 4. Similar to Li_2BeH_4,[16] α-Na_2BeH_4 also exhibits a nonmetallic character of about 4.2 eV energy gap between the valence band (VB) and conduction band (CB). The VB region is split into two separate subbands marked as regions I and II. In region II close to the Fermi energy level E_F, the Be p states and the H s states are energetically degenerate, which facilitates the Be-H hybridization and, thus, the formation of covalently bonded BeH_4 tetrahedron subunits in the crystal. The contribution of the Na s,p states to them is considered to be negligible.

To get a better understanding of the local bonding between H, Be, and Na atoms, the electron localization

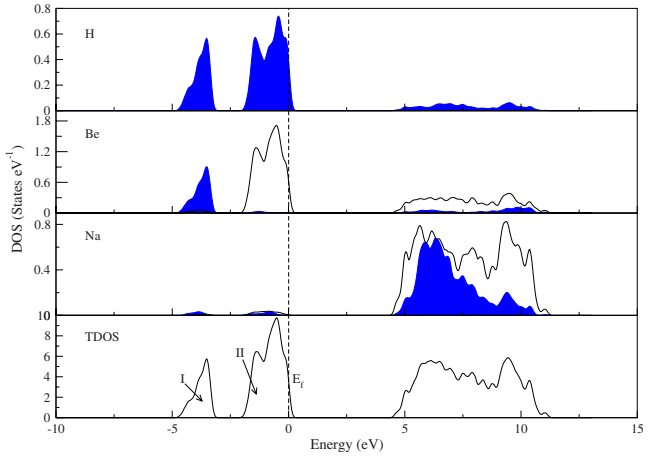

FIG. 4. (Color online) Calculated total and partial electronic densities of states (DOSs) for α-Na_2BeH_4 (at equilibrium). The Fermi energy level E_f is set to zero and marked by a vertical line. The s states are depicted as shaded blue curves.

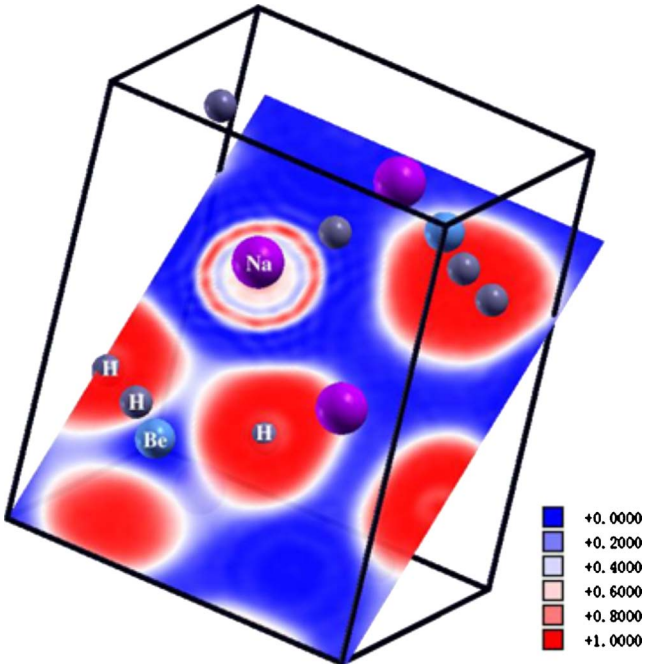

FIG. 5. (Color online) Calculated ELF for α-Na_2BeH_4.

function[43] (ELF) for α-Na_2BeH_4 was further calculated using the PWSCF code.[24] According to its definition, the value of ELF is limited to the range from 0 to 1. The high ELF can be simply interpreted as covalent interaction and the low ELF corresponds to ionic interaction between unpaired electrons. From the calculated ELF displayed in Fig. 5, it can be clearly seen that the high ELF close to 1 is present along the Be-H bonds, which is mainly ascribed to the strong hybridization of the Be p and H s states, consistent with the above DOS analysis. The negligible ELF confirms that the ionic bonding exists between BeH_4^- and Na^+.

One unanswered but important question is whether the $\alpha \rightarrow \beta$ structural transition can also occur with increasing temperature. Performing the phonon calculation based on DFPT[23] and investigating their thermodynamic properties can give us a satisfactory answer. The calculated phonon DOS (PDOS) for α- and β-Na_2BeH_4 are shown in Fig. 6. We can find that the PDOS of α-Na_2BeH_4 is mainly grouped into three frequency bands: (i) low-frequency band below 590 cm^{-1} dominated by motion of the Na and Be ions, (ii) medium-frequency (MF) band between 867 and 1050 cm^{-1} resulting from the H-Al-H bond bending in the corner-sharing BeH_4 tetrahedra, and (iii) high-frequency band above 1510 cm^{-1} mainly being ascribed to the Be-H bond stretching. The main difference in the PDOS of the two phases is that the MF band for α-Na_2BeH_4 is split into two subbands, indicating that rotation of bonds is restrained. The force constant in the BeH_4 subunits is larger for α-Na_2BeH_4 than for β-Na_2BeH_4, implying that α-Na_2BeH_4 would be more stable than β-Na_2BeH_4.

Combining the results of the quasiharmonic approximation (QHA), the thermodynamic properties like the Helmholtz free energies (F) and vibrational entropies (S) are further considered. As shown in Fig. 7, the zero point energies

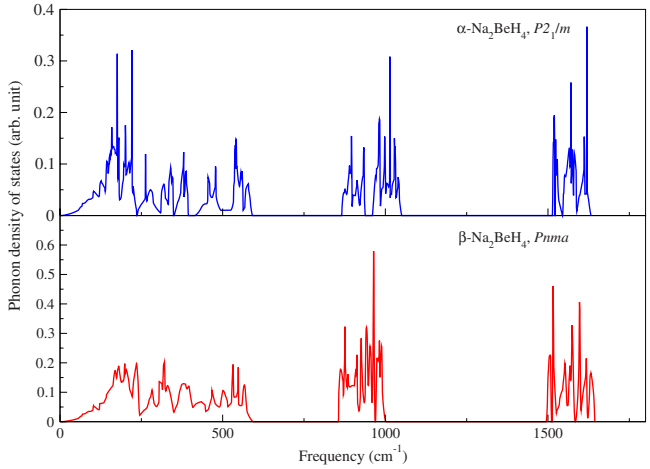

FIG. 6. (Color online) Calculated phonon DOS for α- and β-Na_2BeH_4 at ambient pressure. The PDOSs have been normalized to be $\int g(\omega)d\omega = 3N$.

(ZPEs) of α- and β-Na_2BeH_4 are 0.909 and 0.962 eV/f.u., respectively, considerably larger than those of conventional metal hydrides [for example, the ZPE of TiH_2 is 0.51 eV/f.u. (Ref. 44)]. Their ΔF at $T=0$ K (ΔF_0) reaches about 132.6 cal/mole ($\approx$0.081 eV/f.u.), about four-fifths of their ZPE differences. This means that the ZPE correction is more important in determining the thermal stabilities of Na_2BeH_4. The free energy differences (ΔF) in Fig. 7 show that F of α-Na_2BeH_4 becomes lower and lower than β-Na_2BeH_4 with increasing temperature. The higher ZPE of β-Na_2BeH_4 would make this phase less stable. From the calculated entropies shown in the inset of Fig. 7, it can be found that in the temperature range from 0 to 800 K, the entropic contribution to the free energy is considerably larger for α-Na_2BeH_4($-TS_\alpha$) than for β-Na_2BeH_4($-TS_\beta$). These two factors would be the main reason why α-Na_2BeH_4 is kept more stable than β-Na_2BeH_4 with increasing temperature.

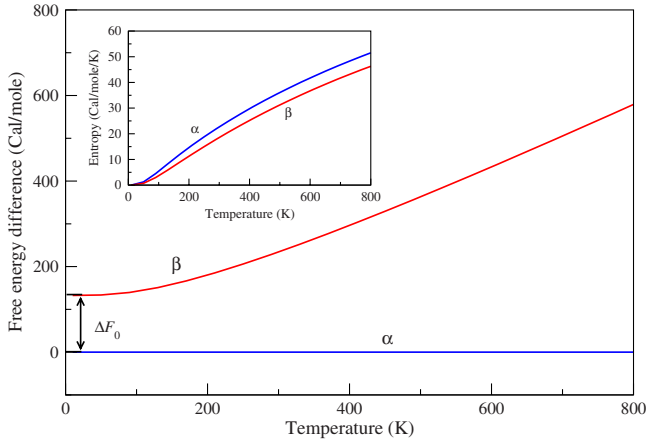

FIG. 7. (Color online) Relation of free energy difference (ΔF) versus temperature (T) for α- and β-Na_2BeH_4. ΔF_0 = 132.6 cal/mol is the free energy difference at $T=0$ K including the zero point energies. The temperature dependence of the vibrational entropy is presented in the inset.

Consequently, we could conclude that the structural transition from α to β phase cannot emerge.

From the viewpoint of crystal chemistry, it is easy to understand the transition from a low-symmetry to a high-symmetry structure. In fact, the phase transition from a monoclinic to an orthorhombic structure with increasing pressure or decreasing temperature has been observed in the experimental studies on some A_2BX_4 compounds including the BX_4 tetrahedral subunits such as Cs_2MoS_4 (Ref. 45) and Cs_2HgCl_4.[46] For α-Na_2BeH_4, with the low-symmetry monoclinic structure, the interatomic distances between Be-H in BeH_4 subunits range from 1.420 to 1.451 Å and the bond angles between H-Be-H range from 105.9° to 112.6°. However, for β-Na_2BeH_4, with the orthorhombic symmetry, the Be-H spacings range from 1.429 to 1.439 Å and the H-Be-H angles range from 107.2° to 111.4°. As being pointed out by C. N. R. Rao and K. J. Rao,[47] increasing temperature generally leads to a low-temperature phase transforming into a phase with larger openness. Being contrary to the factor of temperature, increasing pressure is generally in favor of the transformation from a low-symmetry structure to a high-symmetry structure. Thus, the appearance of the pressure-induced $\alpha \rightarrow \beta$ structural transition should be believable as proposed by Pauling.[11]

IV. CONCLUSIONS

In conclusion, the investigation on the structural, electronic, and thermodynamic properties of Na_2BeH_4 has been performed by using the first-principles total-energy calculations based on DFT. The total-energy calculations on the proposed structures show that at ambient conditions, the crystal structure of α-Na_2BeH_4 belongs to the α-K_2ZnBr_4-type monoclinic structure (space group $P2_1/m$). With increasing pressure, the structural transformation from α- to β-Na_2BeH_4 (α-Cs_2MgH_4 type, space group *Pnma*) occurs at 1.1 GPa, associated with a volume reduction of 8.7%. The DOS and ELF analyses demonstrate that the stronger covalent-bonding interaction prevails in BeH_4 subunits in Na_2BeH_4, and they exhibit a nonmetallic feature. With the use of the QHA, the relative thermal stability of α phase to β phase is further investigated by performing phonon calculations based on DFPT. The calculated Helmholtz free energies and vibrational entropies show that with increasing temperature, α-Na_2BeH_4 is always kept more stable than β-Na_2BeH_4 and, thus, it is impossible to cause a structural transition from α to β phase, which could be conceptually understood from the viewpoint of crystal chemistry.

ACKNOWLEDGMENTS

The authors gratefully thank E. Isaev for helpful discussions on the phonon calculation. The present work was supported by the National Natural Science Foundation of China through Grant No. 50771095.

*Corresponding author. FAX: +86-24-23891320; ymwang@imr.ac.cn

[1] L. Schlapbach and A. Züttel, Nature (London) **414**, 353 (2001).
[2] B. Bogdanovic and M. Schwickardi, J. Alloys Compd. **253-254**, 1 (1997).
[3] A. Zaluska, L. Zaluski, and J. O. Ström-Olsen, J. Alloys Compd. **298**, 125 (2000).
[4] K. J. Gross, E. H. Majzoub, and S. W. Spangler, J. Alloys Compd. **356-357**, 423 (2003).
[5] A. Aguayo and D. J. Singh, Phys. Rev. B **69**, 155103 (2004).
[6] Z. Lodziana and T. Vegge, Phys. Rev. Lett. **93**, 145501 (2004).
[7] J. A. Ritter, A. D. Ebner, J. Wang, and R. Zidan, Mater. Today **6**, 18 (2003).
[8] B. M. Bulychev, R. V. Shapanchenko, E. V. Antipov, D. V. Sheptyakov, S. N. Bushmeleva, and A. M. Balagurov, Inorg. Chem. **43**, 6371 (2004).
[9] N. A. Bell and G. E. Coates, J. Chem. Soc. **1965**, 692.
[10] A. W. Overhauser, Phys. Rev. B **35**, 411 (1987).
[11] L. Pauling, *Linus Pauling Research Notebooks*, http://osulibrary.orst.edu/specialcollections/rnb/36/36-099.html
[12] Y. Liu and M. L. Cohen, Science **245**, 84 (1989).
[13] Chun-gang Duan, W. N. Mei, Jianjun Liu, Wei-guo Yin, J. R. Hardy, R. W. Smith, M. J. Mehl, and L. L. Boyer, Phys. Rev. B **69**, 033102 (2004).
[14] O. M. Løvvik, Phys. Rev. B **71**, 144111 (2005).
[15] B. Magyari-Köpe, V. Ozoliņš, and C. Wolverton, Phys. Rev. B **73**, 220101(R) (2006).
[16] C. H. Hu, D. M. Chen, Y. M. Wang, D. S. Xu, and K. Yang, Phys. Rev. B **75**, 224108 (2007).
[17] D. Vanderbilt, Phys. Rev. B **41**, 7892 (1990).
[18] M. D. Segall, P. L. D. Lindan, M. J. Probert, C. J. Pickard, P. J. Hasnip, S. J. Clark, and M. C. Payne, J. Phys.: Condens. Matter **14**, 2717 (2002).
[19] J. P. Perdew, J. A. Chevary, S. H. Vosko, K. A. Jackson, M. R. Pederson, D. J. Singh, and C. Fiolhais, Phys. Rev. B **46**, 6671 (1992).
[20] D. M. Ceperley and B. J. Alder, Phys. Rev. Lett. **45**, 566 (1980).
[21] J. P. Perdew and A. Zunger, Phys. Rev. B **23**, 5048 (1981).
[22] T. H. Fischer and J. Almlof, J. Phys. Chem. **96**, 9768 (1992).
[23] S. Baroni, S. de Gironcoli, A. dal Corso, and P. Giannozzi, Rev. Mod. Phys. **73**, 515 (2001).
[24] S. Baroni, A. Dal Corso, S. de Gironcoli, P. Giannozzi, C. Cavazzoni, G. Ballabio, S. Scandolo, G. Chiarotti, P. Focher, A. Pasquarello, K. Lassonen, A. Trave, R. Car, N. Marzari, and A. Kokalj, http://www.pwscf.org/
[25] B. Bertheville, P. Fischer, and K. Yvon, J. Alloys Compd. **302**, L12 (2000).
[26] B. Bertheville, P. Fischer, and K. Yvon, J. Alloys Compd. **330-332**, 152 (2000).
[27] P. Seiler, Acta Crystallogr., Sect. B: Struct. Sci. **B49**, 223 (1993).
[28] W. Eysel, H. H. Höfer, K. L. Keester, and Th. Hahn, Acta Crystallogr., Sect. B: Struct. Sci. **41**, 5 (1985).
[29] A. G. Nord, Acta Chem. Scand. (1947-1973) **27**, 814 (1973).
[30] A. S. Koster, F. X. N. M. Kools, and G. D. Rieck, Acta Crystal-

logr., Sect. B: Struct. Crystallogr. Cryst. Chem. **25**, 1704 (1969).
[31] P. M. Skarstad and S. Geller, Mater. Res. Bull. **10**, 791 (1975).
[32] F. S. Galasso, *Structure and Properties of Inorganic Solids* (Pergamon, New York, 1970).
[33] J. Fabry, T. Breczewski, F. J. Zuniga, and A. R. Arnaiz, Acta Crystallogr., Sect. C: Cryst. Struct. Commun. **49**, 946 (1993).
[34] E. G. Moroni, G. Kresse, J. Hafner, and J. Furthmüller, Phys. Rev. B **56**, 15629 (1997).
[35] G. Kresse and D. Joubert, Phys. Rev. B **59**, 1758 (1999).
[36] R. M. Martin, *Electronic Structure: Basic Theory and Practical Methods* (Cambridge University Press, Cambridge, 2004).
[37] V. Magnasco, Chem. Phys. Lett. **387**, 332 (2004).
[38] P. Vajeeston, P. Ravindran, R. Vidya, H. Fjellvåg, and A. Kjekshus, Phys. Rev. B **68**, 212101 (2003).
[39] F. Birch, Phys. Rev. **71**, 809 (1947).
[40] C. H. Hu, D. M. Chen, Y. M. Wang, D. S. Xu, and K. Yang, J. Phys.: Condens. Matter **19**, 176205 (2007).
[41] J. D. Jorgensen, Z. Hu, S. Teslic, D. N. Argyriou, S. Short, J. S. O. Evans, and A. W. Sleight, Phys. Rev. B **59**, 215 (1999).
[42] S. Carlson and A. M. K. Andersen, Phys. Rev. B **61**, 11209 (2000).
[43] A. Savin, R. Nesper, S. Wengert, and T. Fässler, Angew. Chem., Int. Ed. Engl. **36**, 1809 (1997).
[44] K. Miwa and A. Fukumoto, Phys. Rev. B **65**, 155114 (2002).
[45] B. Lorenz, I. Orgzall, P. K. Dorhout, C. C. Raymond, K. Brister, K. Weishaupt, R. D'Adamo, and H. D. Hochheimer, Phys. Rev. B **55**, 2800 (1997).
[46] B. Bagautdinov, A. Jobst, J. Ludecke, and S. van Smaalen, Acta Crystallogr., Sect. B: Struct. Sci. **57**, 231 (2001).
[47] C. N. R. Rao and K. J. Rao, *Phase Transitions in Solids-An Approach to the Study of the Chemistry and Physics of Solids* (McGraw-Hill, New York, 1978).